Modeling of Hall thruster lifetime and erosion mechanisms

IEPC-2007-250

Presented at the 30th International Electric Propulsion Conference, Florence, Italy
September 17-20, 2007

Shannon Y. Cheng* and Manuel Martinez-Sanchez†
Massachusetts Institute of Technology, Cambridge, MA, 02139, USA

An axisymmetric hybrid-PIC model of the Hall thruster plasma discharge has been upgraded to simulate the erosion of the thruster acceleration channel, the degradation of which is the main life-limiting factor of the propulsion system. Evolution of the thruster geometry as a result of material removal due to sputtering is modeled by calculating wall erosion rates, stepping the grid boundary by a chosen time step and altering the computational mesh between simulation runs. The code is first tuned to predict the nose cone erosion of a 200W Busek Hall thruster, the BHT-200. Simulated erosion profiles from the first 500 hours of operation compare favorably to experimental data. The thruster is then subjected to a virtual life test that predicts a lifetime of 1,330 hours, well within the empirically determined range of 1,287-1,519 hours. The model is then applied to the BHT-600, a higher power thruster, to reproduce wear of its exit ring configuration over 932 hours of firing. Though some optimized code features remain the same, others need adjustment to achieve comparable erosion results. Better understanding of the physics of anomalous plasma transport and low-energy sputtering are identified as the most pressing needs for improved lifetime models.

I. Introduction

HALL thrusters are used for propulsion tasks such as geosynchronous orbit stationkeeping and other low thrust orbit-adjusting maneuvers. These missions have primarily employed the thruster at a single nominal operating point and require electric propulsion lifetimes of 2000-3000 hours[1] which is easily satisfied by thrusters like the SPT-100 with a 7000 hour lifetime. As confidence in the technology builds, mission planners are investigating the feasibility of expanding the use of Hall thrusters to purposes ranging from interplanetary cargo transfer[2,3] to aerobraking.[4] To succeed at these functions, it may be desirable to throttle the thruster over a range of operating conditions, either varying power or specific impulse. The effect of off-nominal firing on the device's longevity has not been fully characterized, although lifetime is an important design metric that determines the number of thrusters needed for an extended cargo mission or whether the system is a cost-effective propulsion alternative for cost-capped science missions. Oftentimes, life testing done to qualify thrusters focuses on operating at full power in order to maximize propellant throughput in the shortest amount of time possible. However, during the actual mission, this full power mode may not be the primary firing condition and lifetimes could be significantly longer than those predicted by experiment.[5] Clearly it would be prohibitively expensive and time-consuming to experimentally determine the life span of a thruster at every possible operating condition. Thus, the ability to accurately simulate the mechanisms that lead to failure of the thruster as well as how they are affected by differing firing regimes is required from a mission planning standpoint. Another benefit of a computational model for Hall thruster lifetime and erosion mechanisms is its contribution to the design process. Thruster designers need a tool to foresee how changes in their blueprints affect lifetime as running a life test after each design iteration is costly in both time and resources. Having a predictive capability expedites the process by allowing only promising

*Research Assistant, Department of Aeronautics and Astronautics, turtle@alum.mit.edu.
†Professor, Department of Aeronautics and Astronautics, mmart@mit.edu.

concepts to reach the materialized phase. In addition, once a finalized design is established, the simulation can be used to aid in thruster qualification by performing a virtual life test.

II. Lifetime definition

The lifetime of a Hall thruster is mainly limited by the erosion of components protecting its magnetic circuitry from the discharge plasma. Once the magnetic poles are exposed, further degradation or overheating may occur, affecting the nominal magnetic field and consequently the thruster's performance. Accordingly, end of life is declared when the ceramic exit rings in stationary plasma thrusters (SPT-type) or the metal guard rings in thrusters with anode layer (TAL-type) are breached. These two Hall thruster variants and their sensitive components are illustrated in Figures 1 and 2.

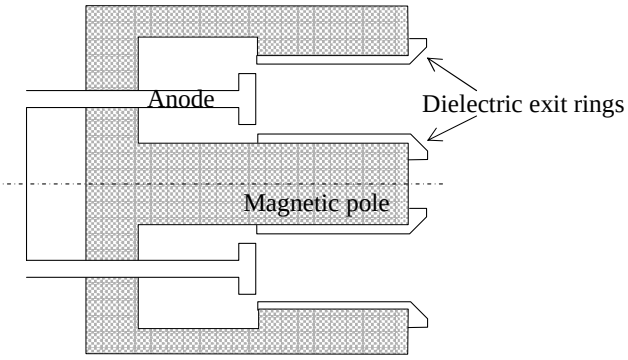

Figure 1. Stationary plasma thruster (SPT).

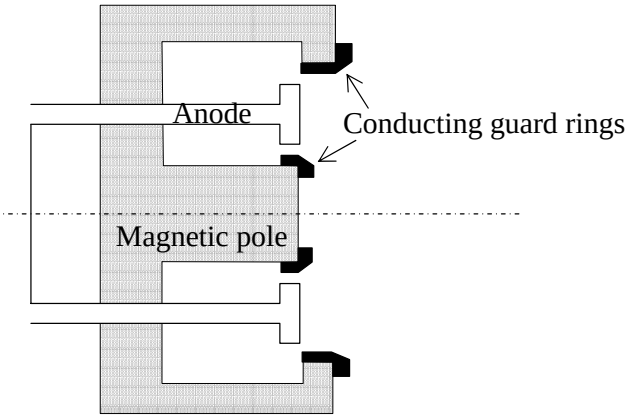

Figure 2. Thruster with anode layer (TAL).

III. Prior work

A. Experimental work

Experiments related to thruster longevity primarily fall into two categories. Long-duration qualification tests aim to directly determine lifetime by operating the thruster for lengthy periods in a continuous fashion.[6–14] Results differ between thrusters, but tests have proven lifetimes on the order of thousands of hours and show that though performance parameters (thrust, efficiency, and specific impulse) may exhibit some variation at the beginning of life, values do not deviate greatly from nominal and tend to stabilize later in life. Asymmetric erosion around the acceleration channel is also commonly observed, but the cause for this azimuthal variation is not well-understood.

In addition to these lengthy tests, shorter experiments have also been performed with the aim of characterizing erosion behavior to allow extrapolation of lifetime. Trials using five different grades of boron nitride exit rings in the laboratory model NASA-120M Hall thruster show significant variation in erosion profiles after 200 hours.[15] Testing of a D-80 in different operating modes for 100 hours proves that erosion is highly dependent on firing condition and exhibits a nonlinear relationship between erosion rate and applied voltage.[16] These results indicate the issue of lifetime prediction is not only thruster-dependent, but also specific to wall material and operating condition.

B. Lifetime prediction models

Besides work done to empirically quantify lifetime and erosion mechanisms of Hall thrusters, development of predictive lifetime models has also been pursued. The basis of all these models gives the wall recession rate as,

$$\xi = j_{iw} S_v(E_i, \theta_i), \tag{1}$$

where j_{iw} is the ion flux to the wall and $S_v(E_i, \theta_i)$ is the volumetric sputtering coefficient which is a function of the target material, the incident ion energy and the ion angle of incidence. Thus, necessary components of any life span forecasting tool are a sputter model for the material in question and a plasma discharge model that gives the wall flux. Though both theoretical and semi-empirical models have been developed to predict Hall thruster lifetime, this summary will focus on reviewing existing computational models.

A number of approaches to numerically simulating the erosion processes in a Hall thruster and their consequences on lifetime have recently emerged. In 2004, Manzella et al.[17] proposed a lifetime prediction model that attributed the mechanism for wall erosion to scattering collisions, arguing that ions impacting the wall must have been diverted from an otherwise uniform plasma flow along the acceleration channel. Building a 1D model around this theory, decent agreement to erosion profiles of the SPT-100 is achieved, but only when the neutral density is increased by a factor of two. Because scattering collisions alone do not produce enough erosion, the assumption of an ideally-focused axial flow is improbable.

Continuing work on this issue, Yim et al. have expanded on these ideas and developed a 2D fluid model more grounded in physics.[18–20] The hydrodynamic description models the plasma species with a finite volume flux-splitting method on an axisymmetric Cartesian mesh. To allow for a changing geometry as the walls erode, a cut cell method is used. In addition to a model for the sputter yield, near-wall scattering collisions are included, ion wall fluxes are given a Maxwellian distribution and the Bohm coefficient is varied to affect the potential profile across the channel. Simulation results tend to underpredict erosion at long times and is weakest at capturing the upstream erosion behavior.

The remaining computational modeling has focused on using 2D hybrid-PIC codes to provide the plasma discharge parameters. In a study to determine the effect of different magnetic field configurations on the SPT-100, Garrigues et al.[21] included a sputtering model to analyze the influence on lifetime. The main conclusion of the analysis confirms the fact that erosion damage to thruster walls decreases when more of the plasma's potential drop occurs outside the channel. This result is already well-understood in the context of TALs which exhibit less erosion than their SPT counterparts due to the acceleration zone being pushed outside the thruster.

Gamero et al. have built upon an existing code, *HPHall*,[22,23] as the foundation of their lifetime prediction capability.[24] Over the course of a simulation run, averaged flux and energy distributions to the channel walls are tracked. During post-processing, these properties are used to generate sputter yields and then erosion rates. Armed with these, the geometry is stepped forward in time and the process is repeated, allowing self-consistent modeling of the geometry evolution. The SPT-100 is used as the test case since erosion profiles over its lifetime are available for direct comparison in the literature.[25] Computational efforts yield results that correctly place the location of channel erosion onset, but overall erosion is under-predicted. Further work on the model is being done to improve neutral injection, wall sheath, and electron mobility modeling with the intent of better matching erosion data.[26,27]

Sommier et al. use a simulation based on *HPHall* as its research base.[28,29] Instead of post-processing with averaged properties, sputtering caused by individual particles crossing the grid boundary is tracked. Neutral sputtering is accounted for, but found to be a factor of 1000 less than that caused by ions. Both charge exchange (CEX) and momentum-exchange ion-neutral collisions are modeled – CEX tends to decrease while momentum-exchange collisions increase erosion. Overall, erosion is decreased by these interactions.

The effect of self-induced magnetic fields is also found to have a minimal effect on the simulation results. Both the Stanford Hall Thruster and SPT-100 are subjected to a virtual life test with the model. Erosion profile data for the Stanford Hall Thruster is unavailable, so only comparison to the SPT-100 profiles gives an indication to the success of the code. As with Gamero's model, Sommier's findings under-predict erosion.

C. Discussion of previous work

Based on the experimental work that has been done in this area, the need for prediction tools is apparent. Full lifetime tests are expensive, time-consuming, and do not cover the entire range of possible operating conditions. Nevertheless, empirical data are crucial for validating proposed models and should be continued. Theoretical models provide a general and simple picture of the erosion issue, but are unlikely to give detailed insight into the thruster-specific problem. Semi-empirical accelerated wear tests attempt to address these concerns, but still involve destruction of a thruster, which may not be desirable in early design stages or if cost is a consideration.

Thus, simulations have the greatest potential to provide a resource-efficient solution as a good model should be able to handle a variety of thruster configurations at different operating conditions. Upon reviewing the current numerical work being done, the greatest roadblock seems to be difficulty in acquiring a complete set of key information needed for successful lifetime modeling. Thruster geometry is usually not a problem, whereas magnetic field configuration is more difficult as these designs are generally proprietary. To model the SPT-100, Gamero and Sommier both used a combination of experimental centerline measurements of the field and a magnetic streamline map from Garrigues that represented the typical configuration. When re-gridding to account for erosion of the walls, assumptions had to be made about the field in the newly exposed regions. As the magnetic field plays a fundamental role in Hall thruster plasma dynamics, it is difficult to expect good results if this input is suspect in any way. Another complication is a lack of understanding of material sputtering behavior at low energy. All the computational models discussed use the same experimental sputter yield data of borosil, the SPT-100 channel ceramic, taken by Garnier.[30] However, the data points are taken at higher energies than those typically seen in a Hall thruster and a method for approximating sputter behavior at low energies is necessary. The approaches taken by the modelers range from logarithmic curve fits to using the form of a theoretical model developed for elemental sputtering. These disparities are further highlighted by an inability to converge on the sputter threshold value, E_{th}, the fundamental parameter of these models. Table 1 illustrates the differences across and sometimes within simulations.

Table 1. Comparison of borosil sputter thresholds used in computational models.

Model	E_{th} (eV)	Reference
Manzella	50	[17]
Yim	50	[18]
	70	[19]
	50, 60, 70	[20]
Garrigues	30-70	[21]
Gamero	56.9	[24]
Sommier	50	[28, 29]

The development of the model in this paper strives to overcome these obstacles by being as detailed as possible in the definition of thruster-specific parameters. Also, when faced with uncertainty in the physics, an effort is made to base the applied solution on solid theory. Two low-power thrusters developed by Busek Co., the BHT-200 and the BHT-600, are studied. These thrusters are chosen because a complete set of data needed for lifetime prediction can be compiled. Geometry and magnetic field information are acquired from Busek Co., sputtering data on the identical grade of channel ceramic have been taken, and erosion profiles for simulation comparison are also accessible. Once the model is tuned for one thruster, its applicability to the other thruster is tested to determine if all appropriate physics affecting erosion has been implemented.

IV. Sputter model

In order to quantify the degradation of Hall thruster lifetime due to erosion of the acceleration channel by the plasma flow, a sputter yield model for the channel material is required. In this paper, the two thrusters considered both have boron nitride (BN) lining their acceleration channels. Boron nitride is an attractive choice for insulation of the magnet poles due to its mechanical strength and thermal shock resistance. In comparison to other insulator materials, BN also exhibits lower erosion rates.

A. Normal yield model

Since available experimental data on boron nitride sputter yields do not address the low-energy regime, where the majority of ions in a Hall thruster fall, the approach is to use an analytical model and rely on experimental data for calibration. It has been seen experimentally that different grades of boron nitride have different sputter properties. As such, in developing the sputter yield model, only data taken by Yalin et al.[31] are used since the BN grade experimented on is identical to that utilized in construction of both the BHT-200 and the BHT-600. The model adapted for use is that of Yamamura et al.[32] who give a theory-based analytical formula that has been empirically tested against available data and is valid for any ion-target combination, though only monatomic targets are included. Following the outlined procedure, the normal sputter yields for boron and nitrogen are calculated and presented in Figure 3. For comparison, Yalin's data as well as the average of the Yamamura-predicted B and N yields are also plotted. Although the analytical formula underpredicts the experimental sputter yield, the results are on the same order of magnitude and show reasonable agreement considering the formula is calibrated to monatomic solids.

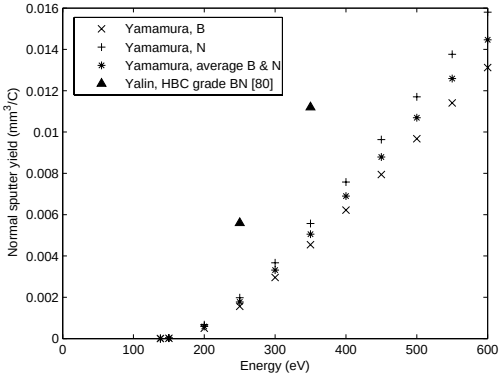

Figure 3. Comparison of $Xe^+ \rightarrow$ BN analytical and experimental normal sputter yields.

The form of Yamamura's formula for normal sputter yield, Y_n, is,

$$Y_n(E) = 0.042 \frac{Q(Z_2)\alpha^*(M_2/M_1)}{U_s} \frac{S_n(E)}{1+\Gamma k_e \epsilon^{0.3}} \left[1 - \sqrt{\frac{E_{th}}{E}}\right]^{2.5}, \quad (2)$$

where E is the energy in eV, E_{th} is the threshold energy in eV, and $Q(Z_2)$, $\alpha^*(M_2/M_1)$, U_s, Γ, and k_e are constants of the projectile-target combination. ϵ is the reduced energy and is linear in E for a given projectile-target combination. $S_n(E)$ has an energy dependence defined by an analytical expression based on the Thomas-Fermi potential,

$$s_n^{TF}(\epsilon) = \frac{3.441\sqrt{\epsilon}\, ln(\epsilon + 2.718)}{1 + 6.355\sqrt{\epsilon} + \epsilon(6.882\sqrt{\epsilon} - 1.708)}. \quad (3)$$

Because the constants determined by the projectile-target combination are not known for the BN ceramic, it is desirable to find a fit that incorporates parameters that represent these unknowns. For small values of ϵ, Equation 3 scales $\sim \sqrt{\epsilon}$. Thus, a fit of the form,

$$Y_n(E) = \frac{AE^{0.5}}{1 + BE^{0.3}} \left(1 - \sqrt{\frac{E_{th}}{E}}\right)^{2.5}, \quad (4)$$

is proposed, where A and B are fitting parameters. To test its validity, the approximation is compared to the full expression for boron and nitrogen, since all parameters needed to evaluate Equation 2 are known. These comparisons are given in Figures 4(a) and 4(b) – only the range of low energies relevant to the problem is considered. It is apparent that the fit as given in Equation 4 does not agree well with the Yamamura model curve since the energy dependence of Equation 3 is not adequately captured. However, if the fit exponent is changed to a value of 0.474, excellent matching is achieved for both elements. Thus, the revised fit,

$$Y_n(E) = \frac{AE^{0.474}}{1 + BE^{0.3}} \left(1 - \sqrt{\frac{E_{th}}{E}}\right)^{2.5}, \tag{5}$$

is used.

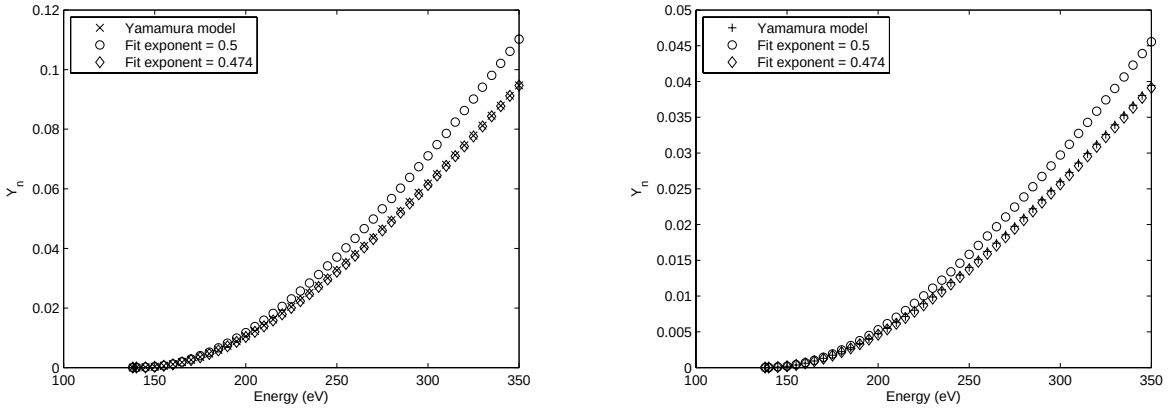

(a) Boron.

(b) Nitrogen.

Figure 4. Comparison of Yamamura model to Equation 4 and 5 approximations.

Using Yalin's boron nitride data, best-fit values of A and B are found for several energy thresholds. These values are given in Table 2. Figure 5(a) plots the yield fit corresponding to a 30 eV energy threshold and Figure 5(b) shows the fits for a range of threshold energies in the near-threshold region. All of these curves pass through Yalin's experimental data points at higher energies. It is apparent that selection of E_{th} is quite important as it can shift the yield curve a significant amount. Since the threshold energy of boron nitride is not known, choice of the appropriate E_{th} is one of the goals of the modeling.

Table 2. Fitted parameters for $Xe^{+}\rightarrow$ BN normal yield approximation.

E_{th} (eV)	A	B
0	0.0000835484	-0.151824
10	0.000164433	-0.146887
20	0.000233999	-0.143251
30	0.000320828	-0.139106
40	0.000436831	-0.133966
50	0.000600157	-0.12718

B. Angular yield model

The angular dependence of the sputter yield is also based on a Yamamura empirical formula.[33] For the case of heavy-ion sputtering, the angular yield has the form,

$$Y_\theta(Y_n, E, \theta_i) = Y_n * cos^{-F}(\theta_i) * e^G, \tag{6}$$

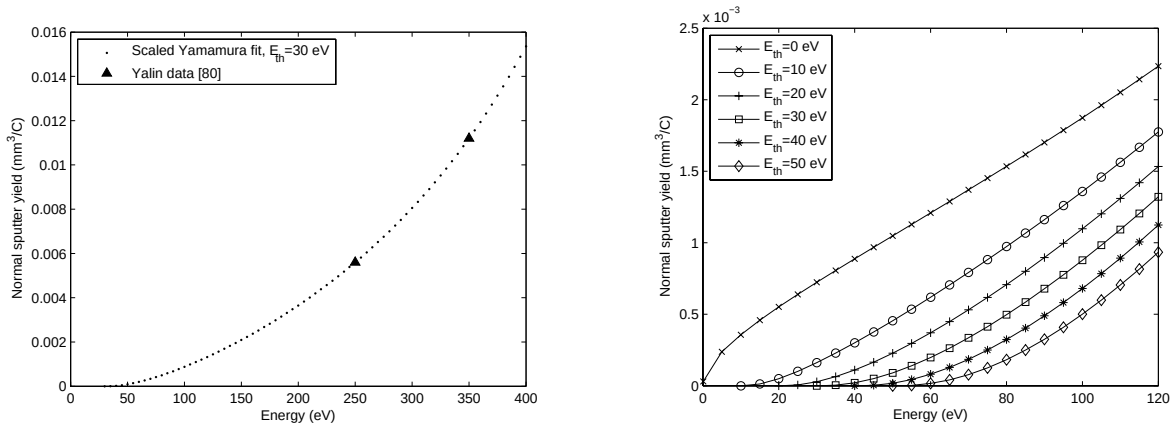

(a) Yield fit for E_{th}=30 eV.

(b) Near-threshold region yield fits.

Figure 5. Yamamura-based normal sputter yield model.

where Y_n is the normal yield, E is the incident energy in eV, θ is the incident angle and F and G are given by,

$$F = -f\left(1 + 2.5\frac{aE^{-1/2}}{1 - aE^{-1/2}}\right),$$

$$G = -\Sigma\left(\frac{1}{cos(\theta_i)} - 1\right),$$

where f, a and Σ are fitting parameters that are tabulated in Table 3. Figure 6 shows the angular yield fits plotted against the experimental data for 250 and 350 eV.

Table 3. Fitting parameters for $Xe^{+}\rightarrow$ BN angular sputter yield formula.

f	5.97563
a	-3.63786
Σ	1.41355

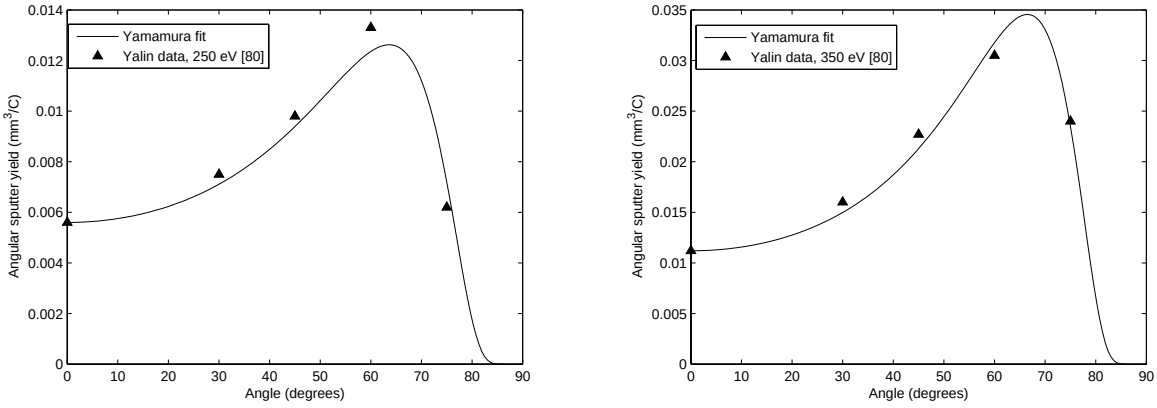

(a) 250 eV.

(b) 350 eV.

Figure 6. Yamamura-based angular sputter yield model.

V. Plasma model

The model of the plasma discharge is based on *HPHall*,[22,23] an existing well-proven Hall thruster simulation. *HPHall* is an axisymmetric model of the area between the anode and cathode. The primary inputs are a two-dimensional (2D) mesh of the simulation region as well as the thruster's magnetic field. Since induced magnetic fields are ignored, this $\vec{B}$ field is considered static. In a balance between detailed physics and heavy computational burden, a hybrid-PIC approach is taken – namely, the heavy ion and neutral species are modeled as discrete particles while the light electrons are represented as a fluid. An assumption of quasineutrality, $n_i = n_e$, links the ion and electron submodels through their densities and further reduces required effort by allowing grid spacings larger than the Debye length. Because the non-neutral wall sheaths are not resolved, an analytic model satisfying the Bohm condition is imposed at relevant grid boundaries to include their effect.[34]

To better capture the evolving wall boundary, an overhaul of the particle mover to rigorously follow the heavy species is implemented to allow accurate tracking of ions as they leave the simulation domain. Individual ions that cross the grid boundary where ceramic is located cause sputtering and contribute to the thruster's erosion. Using the particle's incident energy and angle, which are determined by the plasma potential and wall sheath, the volumetric amount of material sputtered is calculated using the model of the previous section. This yield is then converted to an equivalent erosion depth which is tracked at wall boundary nodes. After running the simulation for an appropriate amount of time, an erosion rate at each wall node can be calculated and the boundary is advanced forward in time to the next iteration. The geometry and corresponding magnetic field are recalculated and the procedure is repeated until the desired number of hours of operation have been achieved. Figure 7 shows the procedural flow chart for modeling the thruster erosion.

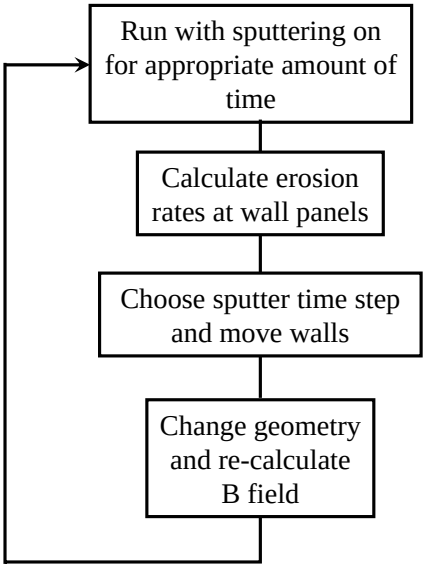

Figure 7. Erosion model flow chart.

Anomalous transport is modeled in *HPHall* by including a constant term in the cross-field electron mobility to represent the greater-than-classical diffusion observed in Hall thrusters,

$$\mu_{e,\perp} = \frac{\mu_e}{\beta_e^2} + K_B \frac{1}{16B}, \tag{7}$$

where $\mu_e = e/\nu_{en} m_e$ is the electron mobility, $\beta_e = \omega_c/\nu_{en}$ is the electron Hall parameter and K_B is the Bohm coefficient. K_B is a parameter adjustable between 0 and 1 and is used to tune the code. However, experimental evidence shows that the anomalous electron mobility is highly correlated with the $E \times B$ drift velocity shear, giving rise to a transport barrier near the exit channel of the thruster.[35] The exact definition of the physics describing this behavior is a topic still under investigation,[36,37] but is beyond the

scope of this work to explore. Nevertheless, the effect exists and is important in determining the nature of the plasma discharge and subsequently its erosion of the channel walls. Thus, a method is implemented to manually impose a transport barrier in an educated manner, a technique that has been successful with other thruster models.[38–40] The imposed transport barrier is specified by prescribing a range of axial coordinates in which the anomalous Bohm diffusion is quenched, or where only classical transport is applied. Outside of the barrier, the usual method of adding the constant Bohm coefficient to the classical contribution of the electron mobility is followed. The exact location and thickness of the barrier is thruster-dependent and without further information requires tuning.

VI. BHT-200 results

The BHT-200, pictured in Figure 8, is a low power Hall thruster developed by Busek Co. Its nominal specifications are summarized in Table 4.[41] A series of experimental nose cone profiles taken in 100 hour increments during the first 500 hours of thruster life is available for comparison to simulation results. An optical comparator, with an estimated error of ±0.127 mm, was used to take the measurements.

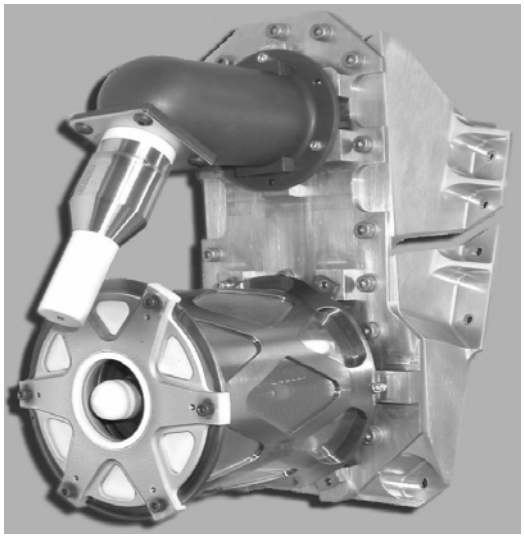

Figure 8. BHT-200 thruster.

Table 4. BHT-200 nominal specifications.

Discharge input power	200 W
Discharge voltage	250 V
Discharge current	0.8 A
Propellant mass flowrate	0.94 mg/s
Thrust	12.8 mN
Specific Impulse	1390 s
Propulsive efficiency	43.5%

The 53×22 computational mesh is based on the thruster geometry depicted in Figure 9. The inner nose cone is made of HBC grade BN and its erosion is the lifetime-limiting factor of the engine. Figure 10 shows a detail of the mesh near the nose cone – the numbered panels are those subject to sputtering and will move as the ceramic erodes. The magnetic field on this and subsequent grids is interpolated from the designed field.

Each simulated lifetime increment requires three *HPHall* runs. To fill the grid with neutrals, 20,000 iterations of NEUTRALS_ONLY mode are performed. Next, 1,400 iterations in NORMAL (all plasma species simulated) mode are used to bypass an initial transient the code exhibits before settling into steady thruster

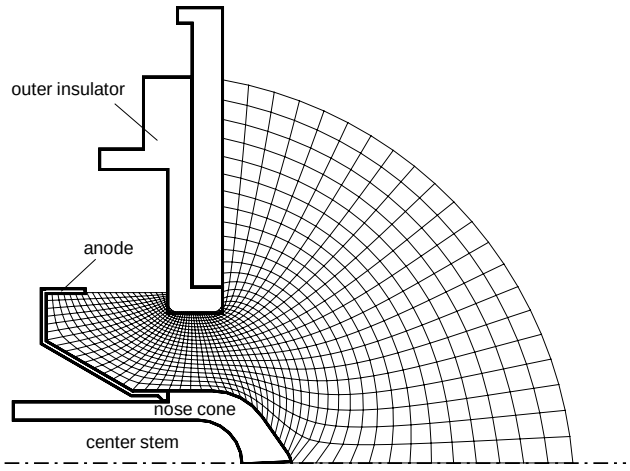

Figure 9. Initial BHT-200 geometry.

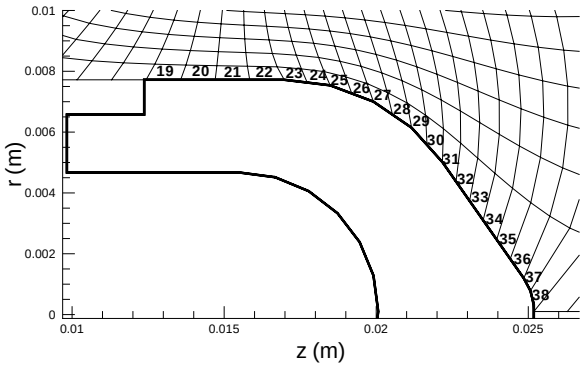

Figure 10. Detail of BHT-200 nose cone panels.

operation. Finally, a longer run in NORMAL mode is done to establish a profile of wall erosion rates at this point in the thruster's life. For the BHT-200 geometry, these runs are performed for 20,000 iterations since its choice is a good compromise between reaching the steady-state erosion rates and having reasonable run times. All runs use an iteration time step of 5×10^{-8} s.

Extensive tuning of the simulation to the erosion profiles from the first 500 hours of operation is performed to determine model inputs.[42] It is found that a sputter threshold of 30 eV, inclusion of double ions, a Bohm coefficient of 0.15, an imposed transport barrier between z=0.015-0.0175 m, and a sputter time step of 100 hours give the best comparison. Figure 11 shows the evolution of the wall profile. Erosion is generally well predicted, though the simulation begins to deviate from experiment in the downstream region later in time. These input parameters are then used to run a simulated life test. Continuing from the accumulated 500 hours of simulated operation, the thruster is stepped in 100 hour increments until 900 cumulative hours are reached. Beyond 900 hours, the time step between runs is selected on a case-by-case basis to better capture the wall evolution, but never exceeds 100 hours. In total, 15 runs are carried out and the thruster first breaks through to the center stem at a time of 1,330 hours and at an axial location of $z \sim 0.01825m$. Figure 11(f) shows the end of life profile. The simulated discharge current is 0.707 A and simulated thrust is 10.934 mN.

The BHT-200 that underwent 500 hours of experimental life testing at Busek was subsequently sent to AFRL at Edwards for completion of the long duration test. In total, the thruster was run for 1700+ hours before the test was voluntarily terminated. Unfortunately, the experiment was not interrupted to take erosion profiles at intermediate times and there is no further data to compare to. However, visual observations were made of the nose cone tip falling off that bracketed the insulator breach to occur between 1,287 and 1,519 hours of thruster firing, putting the simulated lifetime of 1,330 hours in the correct range.

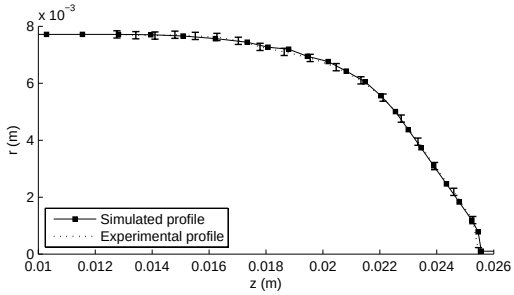

(a) 100 hours.

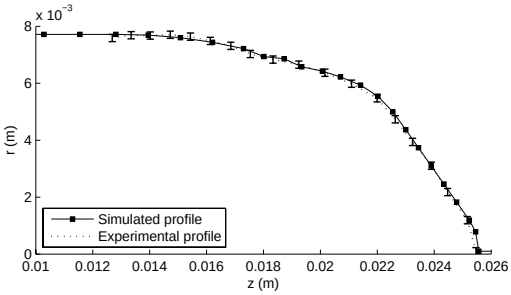

(b) 200 hours.

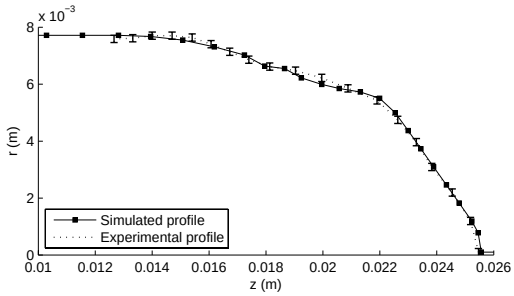

(c) 300 hours.

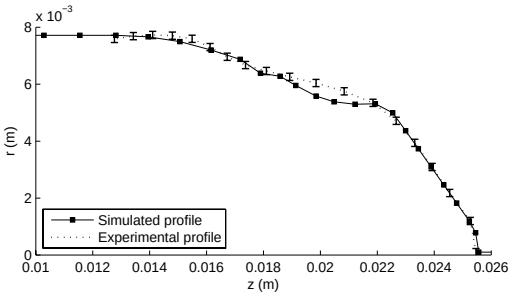

(d) 400 hours.

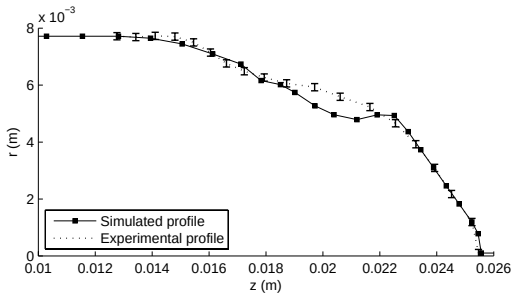

(e) 500 hours.

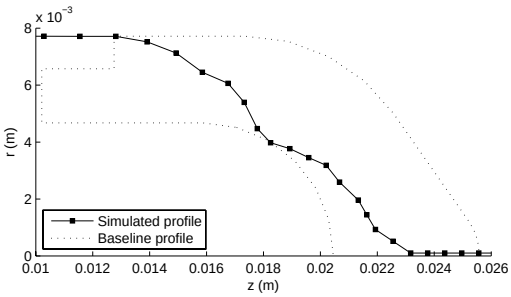

(f) End of life profile (1,330 h).

Figure 11. BHT-200: Erosion profile evolution.

Table 5. BHT-600 nominal specifications.

Discharge input power	600 W
Discharge voltage	300 V
Discharge current	2.05 A
Propellant mass flowrate	2.6 mg/s
Thrust	39.1 mN
Specific Impulse	1530 s
Propulsive efficiency	49.0%

VII. BHT-600 results

The BHT-600 is another member of the low-power Hall thruster family developed at Busek Co. and is pictured in Figure 12. Its nominal specifications are summarized in Table 5.[41] Being larger in size, the BHT-600 forgoes a nose cone in favor of the more traditional exit ring configuration. Wall erosion profiles taken during life testing at Edwards Air Force Base are available for tuning of the code. Experimental profiles were taken using optical profilometry at 80, 225, 368, 494, 665 and 932 hours of thruster operation.

Figure 12. BHT-600 thruster.

The 63×27 computational mesh is based on the thruster geometry depicted in Figure 13(a). Both the inner and outer exit rings are made of HBC grade BN, the same ceramic used for the BHT-200 nose cone. The BHT-600 thruster used for the life test arrived at Edwards having already been operated for 80 hours. During this initial period, a variety of operating conditions were used as well as the cathode being moved further from the discharge chamber. All these changes undoubtedly have an effect on the erosion. Accordingly, as shown in Figure 13(b), the baseline mesh is based instead on the 80 hour erosion profile since the thruster operating parameters were kept constant from this point on in the life test.

As before, each simulated lifetime increment requires three *HPHall* runs. The initial sequence is identical to that of the BHT-200 – 20,000 iterations of NEUTRALS_ONLY mode are followed by 1,400 iterations in NORMAL mode. The long NORMAL mode runs to establish wall erosion rates are performed for 10,000 iterations. Less iterations are required for the BHT-600 geometry since it is less complex than that of the BHT-200 and reaches its final state sooner.

Based on experience with the BHT-200, a sputter threshold of 30 eV, inclusion of double ions, and sputter time steps less than 100 hours are maintained. A Bohm coefficient of 0.20 and an imposed transport barrier between z=0.003-0.0045 m are used. Figure 14 shows results at 494 and 932 hours of operation. The simulation tends to over-predict erosion ahead of the exit ring chamfer and under-predict along the chamfer. Results do capture the higher erosion rates observed on the inner insulator. The simulated discharge current is 1.975 A and the simulated thrust is 30.529 mN.

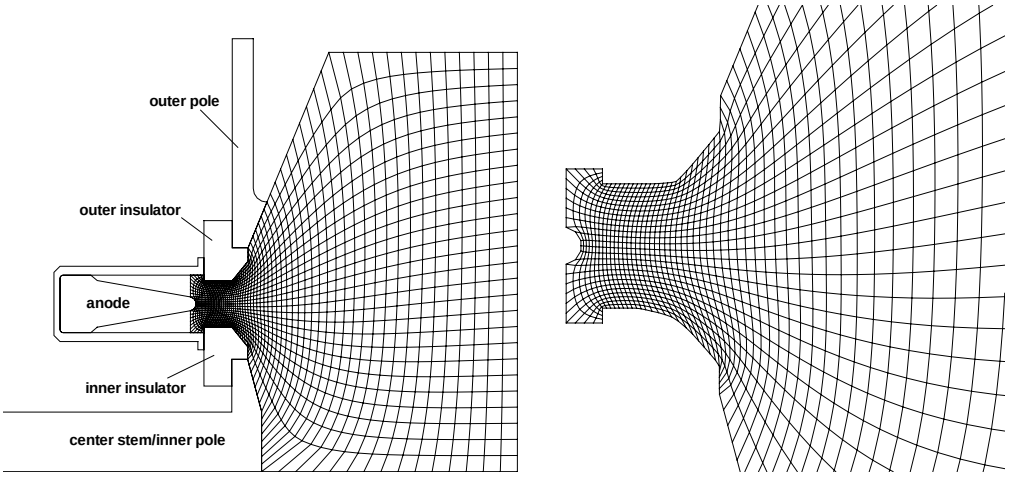

(a) Geometry. (b) 80 hours baseline mesh detail.

Figure 13. BHT-600 mesh.

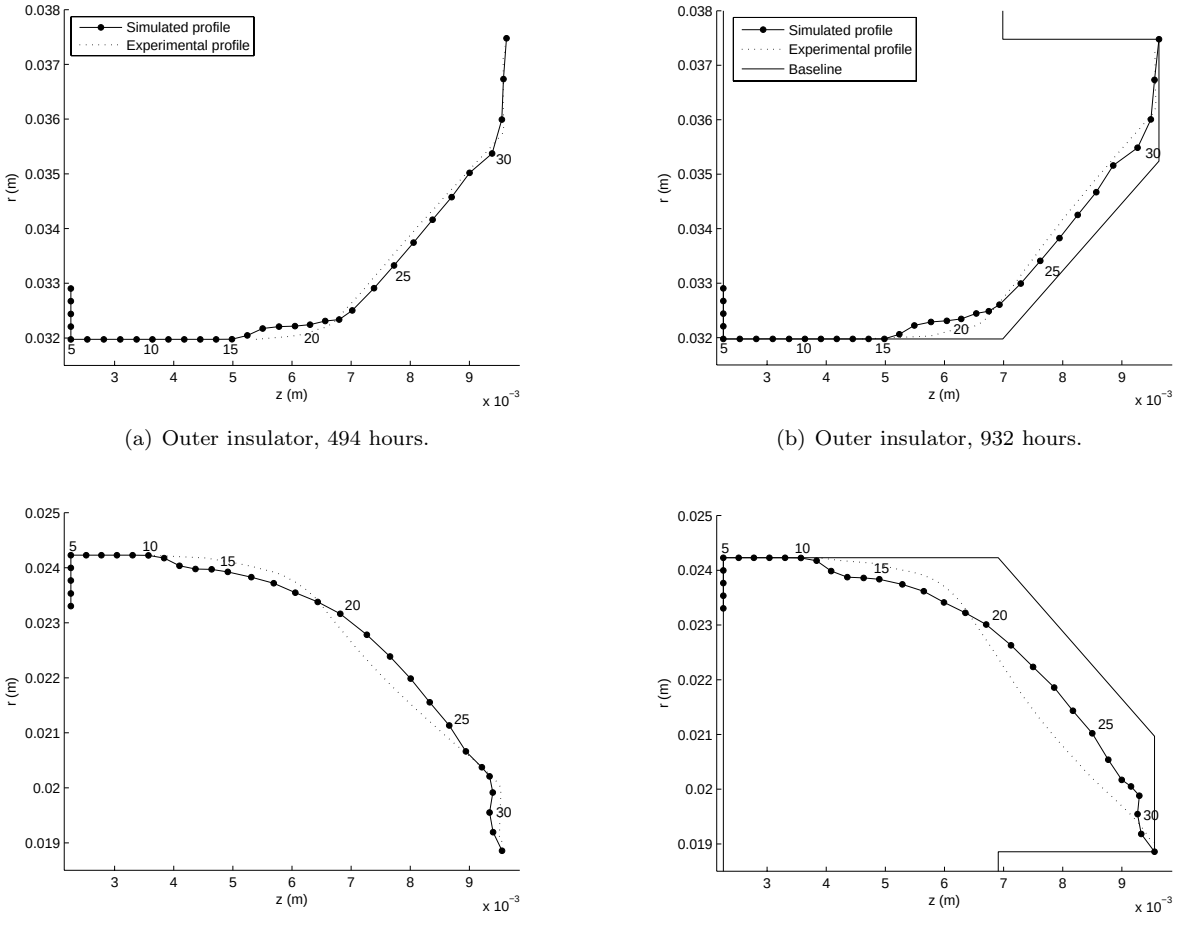

(a) Outer insulator, 494 hours. (b) Outer insulator, 932 hours.

(c) Inner insulator, 494 hours. (d) Inner insulator, 932 hours.

Figure 14. BHT-600: Erosion profile evolution.

VIII. Discussion

The problem of Hall thruster lifetime prediction has been addressed by developing a computational method and testing it against two thruster geometries with empirical data available for comparison. Though the model does not exactly reproduce experimental erosion profiles, it does provide wall regression rates of the right order throughout the thruster's lifetime. As a result, overall agreement of the channel evolution is achieved.

It is observed that the erosion behavior of the two thrusters studied is quite different. In the BHT-200, the majority of the wear occurs prior to the bending of the nose cone away from the channel centerline. The BHT-600, however, exhibits greatest erosion along the chamfer of its exit rings. Because of this difference, it is found that the erosion rates in the 200W thruster closely track the energy of the incoming ions, which has approximately equal kinetic (from acceleration through the potential drop) and potential (from the fall through the wall sheath) contributions. Flux is not a strong erosion indicator as most of the wear occurs in a region where the number of impacting particles exceeds a certain threshold. On the other hand, in the 600W thruster, the erosion rates are determined by both the flux and energy since the bulk of the degradation occurs in an area that is harder for the plasma to reach. Thus, specific tuning of the anomalous transport model is needed for each thruster to place the discharge correctly. Double ions also play an important role in the thruster erosion – in the BHT-200, they account for less than 10% of the wall flux, but increase erosion rates by a factor of 1.5-2. In the BHT-600, double ions are less than 5% of the wall flux, but can increase erosion by a factor as high as 2-2.5.

As evidenced in the work with the BHT-200, it is possible to tune the simulation to a shorter test and then complete the life test numerically. The short-duration test should be long enough that a reasonable amount of wall material has been removed. For the BHT-200, 300 hours is sufficient. When the same approach is applied to the BHT-600, reasonable agreement is achieved with the later profiles, but more work on the transport model is needed to correctly place the plasma in the discharge channel. Nevertheless, features observed during the early stages of the simulation are carried through the virtual lifetime test. Thus, matching of profiles early in life would lead to accurate predictions of those later in life. A cautionary note should be provided to those attempting to predict the terminal wall profile based on erosion rate measurements from the start of thruster life. Figure 15 compares projected wall profiles of the BHT-200 at 1,330 h when erosion rates from 500 h and 1,270 h are used. The two projections give quite different views on the thruster state at this point. At 1,330 hours, the projection from 500 h has already broken through the nose cone to the center stem and the thruster end of life (EOL) would have been earlier. Furthermore, the location of the breach would have been further downstream. It can be seen that the time-dependence of the erosion rates due to the gradual exposure of the nose cone tip to the plasma is not captured as it remains uneroded.

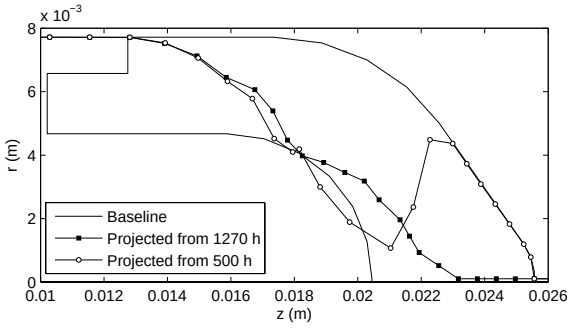

Figure 15. BHT-200 projected end of life profiles (1,330 h).

Despite the model's success at capturing erosion behavior, it is deficient at simultaneously reproducing performance parameters. Cases that agree better with nominal discharge current and thrust do not necessarily correlate with improved wear prediction. Hence, the matching of simulated and experimental bulk properties should not solely be used to calibrate codes as insight into whether the detailed plasma distribution is correct is not provided. Since close attention is paid to the geometry and magnetic field definitions, this shortcoming of the simulation can be attributed to a lack of understanding in the sputter yield and anomalous transport models. By adjusting the sputtering model via the sputter threshold and the

transport model via the Bohm coefficient and transport barrier position, agreement to either the erosion or the performance can be attained. Though tuning was extensive, it was not exhaustive and it is possible the correct combination of parameters could yield success on both metrics. However, the uncertainty in both fundamental physics models suggests further basic research is needed before progressing with the lifetime issue, which is currently an exercise in educated adjustment of parameters. Along with a deeper theoretical insight into the low-energy sputtering and anomalous transport processes, experimental measurements of sputter yield at low energy and internal discharge plasma parameters are key to the continued development of accurate lifetime prediction models. Although the thruster erosion profiles can serve as an interior diagnostic by dispensing clues about the energies of ions flowing to the walls, concrete data such as the potential or plasma density profile along the channel would enable pinning of the computational model to reality.

IX. Conclusion

A multi-scale Hall thruster model that spans time scales on the order of tens of nanoseconds up to hundreds of hours has been developed to predict the erosion mechanisms that determine the lifetime of the device. The attention paid to definition of thruster geometry and magnetic field has eliminated these parameters as sources of error and allows closer examination of possible discrepancies in the underlying physics models. It is found that greater understanding of the mechanisms affecting near-threshold sputtering and anomalous transport is critical to progressing with the problem. By investigating two thrusters with significantly different geometries, the contrast in the evolution of their erosion profiles points to the problem being thruster-specific. Lifetime prediction models must take these disparities into account and generic approaches are not adequate.

References

[1]Vinogradov, V. N., V. M. Murashko and F. Scortecci. "Cost-Optimum Electric Propulsion for Constellations." *Journal of Spacecraft and Rockets*, 39(1):146-149, January-February 2002.

[2]Frisbee, R. H., "Evaluation of High-Power Solar Electric Propulsion Using Advanced Ion, Hall, MPD, and PIT Thrusters for Lunar and Mars Cargo Missions." AIAA-2006-4465, 42^{nd} AIAA/ASME/SAE/ASEE Joint Propulsion Conference and Exhibit, Sacramento, CA, July 2006.

[3]Winski, R., J. Wang, C. Carpenter, J. Cassady and A. Hoskins, "Lunar Robotic Precursor Missions Using Electric Propulsion." AIAA-2006-5165, 42^{nd} AIAA/ASME/SAE/ASEE Joint Propulsion Conference and Exhibit, Sacramento, CA, July 2006.

[4]Hofer, R. R., T. M. Randolph, D. Y. Oh, J. S. Snyder and K. H. deGrys, "Evaluation of a 4.5 kW Commercial Hall Thruster System for NASA Science Missions." AIAA-2006-4469, 42^{nd} AIAA/ASME/SAE/ASEE Joint Propulsion Conference and Exhibit, Sacramento, CA, July 2006.

[5]Dankanich, J. W. and T. Polsgrove, "Mission Benefits of Gridded Ion and Hall Thruster Hybrid Propulsion Systems." AIAA-2006-5162, 42^{nd} AIAA/ASME/SAE/ASEE Joint Propulsion Conference and Exhibit, Sacramento, CA, July 2006.

[6]Garner, C. E., J. R. Brophy, J. E. Polk and L. C. Pless, "A 5,730-Hr Cyclic Endurance Test of the SPT-100." AIAA-1995-2667, 31^{st} AIAA/ASME/SAE/ASEE Joint Propulsion Conference and Exhibit, San Diego, CA, July 1995.

[7]Arkhipov, B., A. S. Bober, R. Y. Gnizdor, K. N. Kozubsky, A. I. Korakin, N. A. Maslennikov and S. Y. Pridannikov, "The Results of 7000-Hour SPT-100 Life Testing." IEPC-1995-39, 24^{th} International Electric Propulsion Conference, Moscow, Russia, September 1995.

[8]Petrosov, V. A., A. I. Vasin, V. I. Baranov, J. R. Wetch, E. J. Britt, S. P. Wong and R. Lin, "A 2000 Hours Lifetime Test Results of 1.3 kW T-100 Electric Thruster." IEPC-1995-41, 24^{th} International Electric Propulsion Conference, Moscow, Russia, September 1995.

[9]Mason, L. S., R. S. Jankovsky and D. H. Manzella, "1000 Hours of Testing on a 10 Kilowatt Hall Effect Thruster." AIAA-2001-3773, AIAA-2001-3351, 37^{th} AIAA/ASME/SAE/ASEE Joint Propulsion Conference and Exhibit, Salt Lake City, UT, July 2001.

[10]Marchandise, F. R., J. Biron, M. Gambon, N. Cornu, F. Darnon and D. Estublier, "The PPS-1350 qualification demonstration 7500h on ground, about 5000h in flight." IEPC-2005-209, 29^{th} International Electric Propulsion Conference, Princeton, NJ, October 2005.

[11]de Grys, K., B. Welander, J. Dimicco, S. Wenzel, B. Kay, V. Khayms and J. Paisley, "4.5 kW Hall Thruster System Qualification Status." AIAA-2005-3682, 41^{st} AIAA/ASME/SAE/ASEE Joint Propulsion Conference and Exhibit, Tucson, AZ, July 2005.

[12]Garner, C. E., J. R. Brophy, J. E. Polk, S. Semenkin, V. Garkusha, S. Tverdokhlebov and C. Marrese, "Experimental Evaluation of Russian Anode Layer Thrusters." AIAA-1994-3010, 30^{th} AIAA/ASME/SAE/ASEE Joint Propulsion Conference and Exhibit, Indianapolis, IN, June 1994.

[13]Semenkin, A., A. Kochergin, A. Rusakov, V. Bulaev, J. Yuen, J. Shoji, C. Garner and D. Manzella, "Development Program and Preliminary Test Results of the TAL-110 Thruster." AIAA-1999-2279, 35^{th} AIAA/ASME/SAE/ASEE Joint Propulsion Conference and Exhibit, Los Angeles, CA, June 1999.

[14]Jacobson, D. T., "High Voltage TAL Erosion Characterization." AIAA-2002-4257, 38^{th} AIAA/ASME/SAE/ASEE Joint Propulsion Conference and Exhibit, Indianapolis, IN, July 2002.

[15]Peterson, P. Y. and D. H. Manzella, "Investigation of the Erosion Characteristics of a Laboratory Hall Thruster." AIAA-2003-5005, 39^{th} AIAA/ASME/SAE/ASEE Joint Propulsion Conference and Exhibit, Huntsville, AL, July 2003.

[16]Solodukhin, A. E. and A. V. Semenkin, "Study of Discharge Channel Erosion in Multi Mode Anode Layer Thruster." IEPC-2003-0204, 28^{th} International Electric Propulsion Conference, Toulouse, France, March 2003.

[17]Manzella, D., J. Yim and I. Boyd, "Predicting Hall Thruster Operational Lifetime." AIAA-2004-3953, 40^{th} AIAA/ASME/SAE/ASEE Joint Propulsion Conference and Exhibit, Fort Lauderdale, FL, July 2004.

[18]Yim, J. T., M. Keidar and I. D. Boyd, "An Evaluation of Sources of Erosion in Hall Thrusters." AIAA-2005-3530, 41^{st} AIAA/ASME/SAE/ASEE Joint Propulsion Conference and Exhibit, Tucson, AZ, July 2005.

[19]Yim, J. T., M. Keidar and I. D. Boyd, "A Hydrodynamic-Based Erosion Model for Hall Thrusters." IEPC-2005-013, 29^{th} International Electric Propulsion Conference, Princeton, NJ, October 2005.

[20]Yim, J. T., M. Keidar and I. D. Boyd, "An Investigation of Factors Involved in Hall Thruster Wall Erosion Modeling." AIAA-2006-4657, 42^{nd} AIAA/ASME/SAE/ASEE Joint Propulsion Conference and Exhibit, Sacramento, CA, July 2006.

[21]Garrigues, L., G. J. M. Hagelaar, J. Bareilles, C. Boniface and J. P. Bouef. "Model study of the influence of the magnetic field configuration on the performance and lifetime of a Hall thruster." *Physics of Plasmas*, 10(12):4886-4892, December 2003.

[22]Fife, J. M., *Two-Dimensional Hybrid Particle-In-Cell Modeling of Hall Thrusters*, SM Thesis, Massachusetts Institute of Technology, May 1995.

[23]Fife, J. M. *Hybrid-PIC Modeling and Electrostatic Probe Survey of Hall Thrusters*, PhD thesis, Massachusetts Institute of Technology, Department of Aeronautics and Astronautics, September 1998.

[24]Gamero-Castaño, M. and I. Katz, "Estimation of Hall Thruster Erosion Using HPHall." IEPC-2005-303, 29^{th} International Electric Propulsion Conference, Princeton, NJ, October 2005.

[25]Absalamov, S. K., V. B. Andreev, T. Colbert, M. Day, V. V. Egorov, R. U. Gnizdor, H. Kaufman, V. Kim, A. Korakin, K. N. Kozubsky, S. S. Kudravzev, U. V. Lebedev, G. A. Popov and V. V. Zhurin, "Measurement of Plasma Parameters in the Stationary Plasma Thruster (SPT-100) Plume and its Effects on Spacecraft Components." AIAA-1992-3156, 28 th AIAA/ASME/SAE/ASEE Joint Propulsion Conference and Exhibit, Nashville, TN, July 1992.

[26]Hofer, R. R., I. Katz, I. G. Mikellides and M. Gamero-Castaño, "Heavy Particle Velocity and Electron Mobility Modeling in Hybrid-PIC Hall Thruster Simulations." AIAA-2006-4658, 42^{nd} AIAA/ASME/SAE/ASEE Joint Propulsion Conference and Exhibit, Sacramento, CA, July 2006.

[27]Hofer, R. R., I. G. Mikellides, I. Katz, and D. M. Goebel, "Wall Sheath and Electron Mobility Modeling in Hybrid-PIC Hall Thruster Simulations." AIAA-2007-5267, 43^{rd} AIAA/ASME/SAE/ASEE Joint Propulsion Conference and Exhibit, Cincinnati, OH, July 2007.

[28]Sommier, E., M. K. Allis and M. A. Cappelli, "Wall Erosion in 2D Hall Thruster Simulations." IEPC-2005-189, 29^{th} International Electric Propulsion Conference, Princeton, NJ, October 2005.

[29]Sommier, E., M. K. Allis, N. Gascon and M. A. Cappelli, "Wall Erosion in 2D Hall Thruster Simulations." AIAA-2006-4656, 42^{nd} AIAA/ASME/SAE/ASEE Joint Propulsion Conference and Exhibit, Sacramento, CA, July 2006.

[30]Garnier, Y., J. -F. Roussel, and J. Bernard. "Low-energy xenon ion sputtering of ceramics investigated for stationary plasma thrusters." *Journal of Vacuum Science and Technology A*, 17(6):3246-3254, November-December 1999.

[31]Yalin, A. P., V. Surla, C. Farnell, M. Butweiller and J. D. Williams, "Sputtering Studies of Multi-Component Materials by Weight Loss and Cavity Ring-Down Spectroscopy." AIAA-2006-4338, 42^{nd} AIAA/ASME/SAE/ASEE Joint Propulsion Conference and Exhibit, Sacramento, CA, July 2006.

[32]Yamamura, Y. and H. Tawara. "Energy Dependence of Ion-Induced Sputtering Yields from Monatomic Solids at Normal Incidence." *Atomic Data and Nuclear Data Tables*, 62(2):149-253, March 1996.

[33]Yamamura, Y. "An Empirical Formula for Angular Dependence of Sputtering Yields." *Radiation Effects and Defects in Solids*, 80(1-2):57-72, February 1984.

[34]Parra, F. I., E. Ahedo, J. M. Fife and M. Martinez-Sanchez. "A two-dimensional hybrid model of the Hall thruster discharge." *Journal of Applied Physics*, 100(2):023304, July 2006.

[35]Cappelli, M. A., N. B. Meezan and N. Gascon, "Transport Physics in Hall Plasma Thrusters." AIAA-2002-0485, 40^{th} AIAA Aerospace Sciences Meeting and Exhibit, Reno, NV, January 2002.

[36]Allis, M. K., C. A. Thomas, N. Gascon, M. A. Cappelli and E. Fernandez, "Introduction of Physical Transport Mechanisms into 2D Hybrid Hall Thruster Simulations." AIAA-2006-4325, 42^{nd} AIAA/ASME/SAE/ASEE Joint Propulsion Conference and Exhibit, Sacramento, CA, July 2006.

[37]Fox, J. M., A. A. Batishcheva, O. V. Batishchev and M. Martinez-Sanchez, "Adaptively Meshed Fully-Kinetic PIC-Vlasov Model For Near Vacuum Hall Thrusters." AIAA-2006-4324, 42^{nd} AIAA/ASME/SAE/ASEE Joint Propulsion Conference and Exhibit, Sacramento, CA, July 2006.

[38]Allis, M. K., N. Gascon, C. Vialard-Goudou, M. A. Cappelli and E. Fernandez, "A Comparison of 2-D Hybrid Hall Thruster Model to Experimental Measurements." AIAA-2004-3951, 40^{th} AIAA/ASME/SAE/ASEE Joint Propulsion Conference and Exhibit, Fort Lauderdale, FL, July 2004.

[39]Fox, J. M., *Parallelization of a Particle-in-Cell Simulation Modeling Hall-Effect Thrusters*, Master's Thesis, Massachusetts Institute of Technology, January 2005.

[40]Koo, J. W. and I. D. Boyd, "Anomalous electron mobility modeling in Hall thrusters." AIAA-2005-4057, 41^{st} AIAA/ASME/SAE/ASEE Joint Propulsion Conference and Exhibit, Tucson, AZ, July 2005.

[41]Hall Effect Thruster Systems: Low Power Nominal Specifications. Busek Co. Inc. 1 May 2007 <http://www.busek.com/halleffect.html>.

[42]Cheng, S. Y. *Modeling of Hall thruster lifetime and erosion mechanisms*, PhD thesis, Massachusetts Institute of Technology, Department of Aeronautics and Astronautics, May 2007.